Electronic Supplementary Material (ESI) for Journal of Materials Chemistry C.

Supporting Information

Large Strain and Temperature-Insensitive Piezoelectric Effect in High-Temperature Piezoelectric Ceramics

Zhuang Liu[1,+], Chunlin Zhao[1,+], Jing-Feng Li[2], Ke Wang[2], and Jiagang Wu*[1,a)]

[1]*Department of Materia ls Science, Sichuan University, Chengdu, 610064, P. R. China*

[2]*Key Laboratory of New Ceramics and Fine Processing, School of Materials Science and Engineering, Tsinghua University, Beijing, 100083, P. R. China*

[+]Equal Contribution

*Corresponding author:

a) mswujg@scu.edu.cn and wujiagang0208@163.com

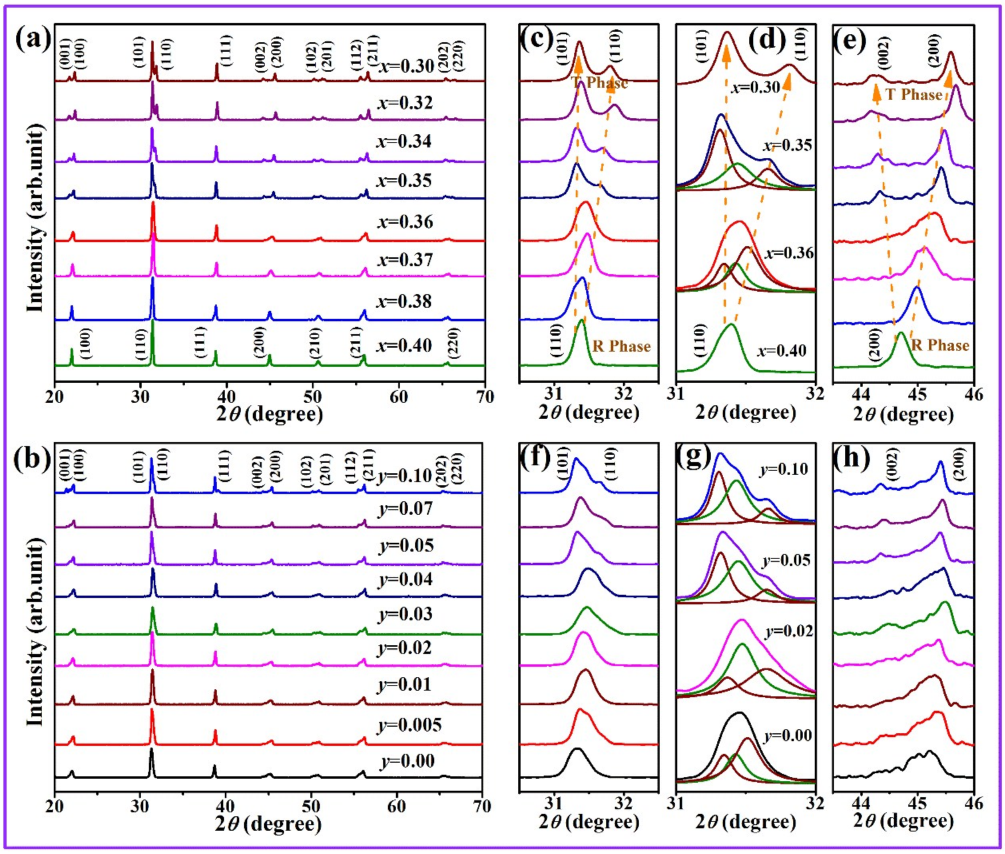

Figure S1. XRD patterns of BS-PT-BZT ceramics with different BS contents: (a) 2θ=20-70^{o}, (c) 2θ=31^{o}-32^{o}, and (e) 2θ=44^{o}-46^{o} and with different BZT contents: (b) 2θ=20-70^{o}, (f) 2θ=31^{o}-32^{o}, and (h) 2θ=44^{o}-46^{o}. And Lorentz fitting curves at 2θ=31^{o}-32^{o} with different (d) BS contents and (g) BZT contents.

Figs. S1 showed the room temperature XRD patterns of BS-PT-BZT ceramics with different BS and BZT contents measured at 2θ=20^{o}-70^{o}. All the ceramics have a pure perovskite structure, indicating that $Bi(Zn_{1/2}Ti_{1/2})O_3$ was crystallized into BS-PT to form the stable solid solution. In addition, the XRD patterns of these samples indicated a phase transition from tetragonal to rhombohedral phase with increasing BS content (x). As shown in Figs. S1(c) and (e), typical rhombohedral phase was observed in the composition range of x=0.37-0.40 and tetragonal phase located at x=0.30-0.35 [1]. The $(101)_T$ and $(110)_T$ peaks around 2θ=31-32^{o} gradually merged to

$(110)_R$ peak with increasing x (0.35~0.37), indicating a phase transformation from tetragonal to rhombohedral phase. Similar results were also observed in diffraction peaks around 2θ=44-45° [Fig. S1(e)]. The $(002)_T$ and $(200)_T$ peaks gradually merged to $(200)_R$-reflection peak with increasing x, suggesting a phase transformation from tetragonal to rhombohedral phase [1-3]. In addition, one can find from Figs. S1(f) and (h) that the peaks at 2θ=31-32° and 44-45° in all samples remained unchanged with increasing BZT contents (0.00~0.10), indicating the construction of R-T MPB phase boundary region. To further confirm the analysis results, the peaks in MPB region were fitted, as shown in Figs. S1(d) and (g). The peaks (2θ=31-32°) in MPB compositions can be fitted by three peaks: $(101)_T$, $(110)_R$, and $(110)_T$, indicating a mixture of rhombohedral and tetragonal phases [2]. Finally, the phase structure of $(1-y)[x\mathrm{BS}-(1-x)\mathrm{PT}]-y\mathrm{BZT}$ ceramics (x=0.35-0.37 and y=0.00-0.10) was identified as R-T MPB region and marked as shadow ellipse. In addition, the T phase gradually increased while R phase was suppressed with the increase of BZT contents [Fig. 1(a)], which well matches with XRD results [Fig. S1]. As a result, the MPB ($0.35 \leq x \leq 0.37$ and $0.00 \leq y \leq 0.10$) can be constructed by modifying the BZT contents.

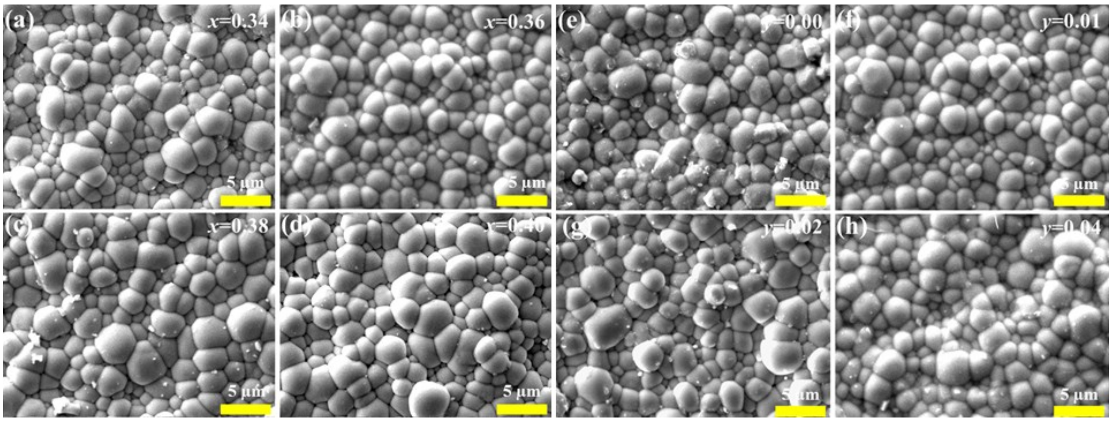

Figure S2. FE-SEM images of the ceramics' surface with various BS contents: (a) x=0.34, (b) x=0.36, (c) x=0.38, (d) x=0.40 and with different BZT contents: (e) y=0.00, (f) y=0.01, (g) y=0.03, (h) y=0.04.

The FE-SEM images from the surface morphologies of the sintered samples were presented in Fig. S2. The spherical grains could be observed in all the samples. Large grains were always surrounded by the small ones, indicating the formation of compact and dense structure during the high-temperature process. In addition, their grain sizes were dependent on the chemical compositions. As shown in Figs. S2(a)-(d), their grain sizes decreased slightly from x=0.34 to x=0.36, and then increased with further increasing x. On the other hand, we also found from Figs. S2(e)-(h) that grain sizes gradually dropped with increasing y and the grains became more uniform for y=0.01. Therefore, the dense microstructure and uniform grain distribution may be beneficial for the enhancement of electrical properties [4-6].

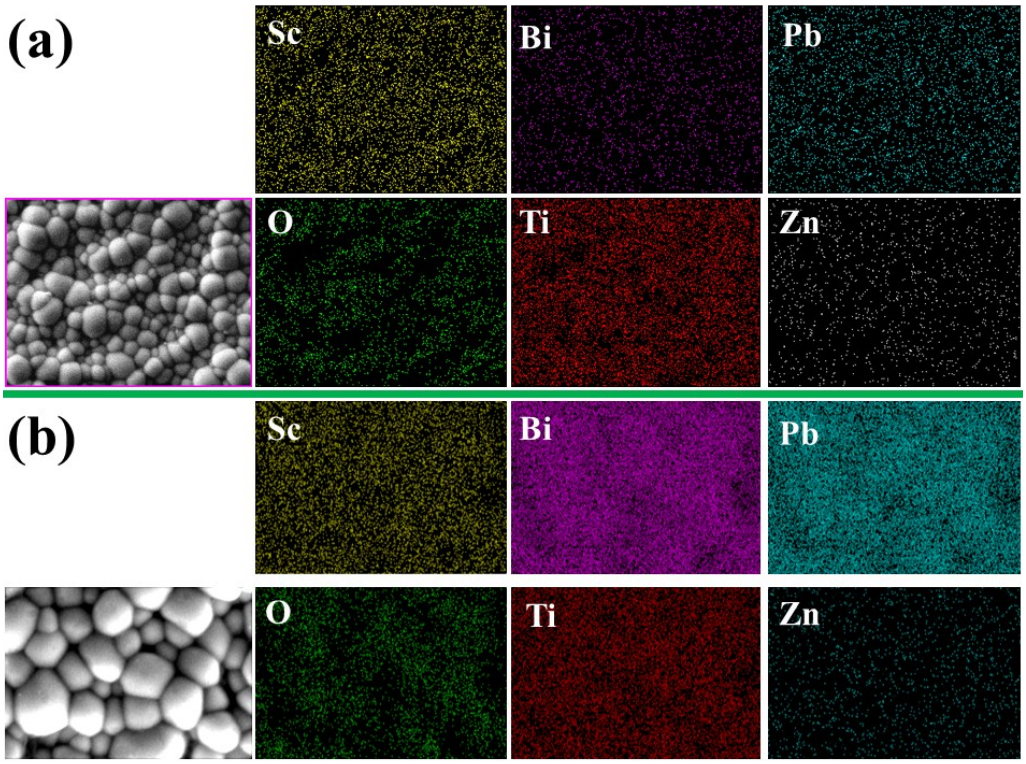

Figure S3. Element mapping and EDX of the ceramics with x=0.36 and y=0.01 under (a) 2000X and (b) 10000X magnification.

To further analyze the elements distribution and confirm the existence of the elements involved, we conducted the element mapping of the ceramics with *x*=0.36 and *y*=0.01 using the EDX analysis under 2000 and 10000 times magnification, as shown in Fig. S3. One can see that all the elements (e.g., Sc, Bi, Pb, Ti, O, and Zn) were found and homogenously distributed in the ceramics. Moreover, we found from Fig. S3(b) that elements were uniformly diffused into samples in spite of that inside grains or in grain boundaries, indicating that there were not elements enriched zones in ceramics, which may also benefit for the enhancement of electrical properties.

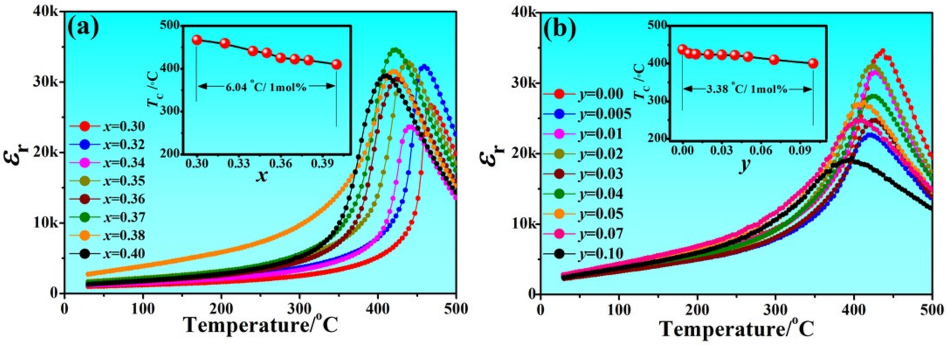

Figure S4. Temperature dependence of dielectric constant (*f*=100 kHz) of (1-*y*)[*x*BS-(1-*x*)PT]-*y*BZT samples with different (a) *x* and (b) *y* contents. The insets in (a) and (b) are their T_C against compositions.

Figure S4 showed the temperature dependence of dielectric constant of (1-*y*)[*x*BS-(1-*x*)PT]-*y*BZT samples with different *x* and *y* contents, measured in the frequency of 100 kHz and 30~500 °C. In addition, the curves of T_C *vs*. the compositions were also exhibited in the insets of Figs. S4(a) and (b). It was found that theirs T_C values decreased slowly from 467 °C to 410 °C and from 437 °C to 400 °C with the increase of BS and BZT contents, respectively. Although their T_C decreased after doping BS or BZT, all the samples maintained a high T_C of >400 °C, which is much higher than those of commercial PZT-based ceramics. To illustrate the descending speed of T_C, the related values were noted in insert charts. Relatively small descent speed could be observed in the ceramics with various x contents (y=0.01) and different y contents (x=0.36), which were 6.04 ^{o}C/1 mol% for the former and 3.38 ^{o}C/1 mol% for the latter. Therefore, high Curie temperature could be found in these ceramics by optimizing the compositions of x and y.

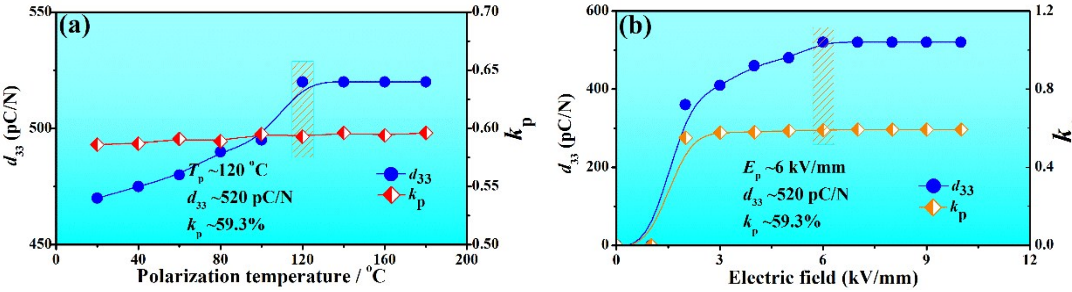

Fig. S5. d_{33} and k_p of the ceramics with x=0.36 and y=0.01 as a function of poling temperatures and electric fields.

According to the previous reports, poling condition (i.e., poling temperature and electric field) is extremely significant for the enhancement of piezoelectric properties [7-8]. In this work, we explored the effects of poling temperature (T_P) and electric field (E_P) on the piezoelectric properties of the ceramics with x=0.36 and y=0.01, as shown in Fig. S5. Figure S5(a) demonstrated piezoelectric coefficient d_{33} and planar electromechanical coupling factor k_p against T_P of the ceramics, measured at E_P=6 kV/mm. It was found that d_{33} increased gradually with the increase of T_P, reached the maximum value of ~520 pC/N under 120 ^{o}C, and remained unchanged with further heating up, indicating that a high T_P can benefit the polarization rotation. However, k_p values were not sensitive to poling temperatures, maintaining a high level of ~59.3%. Figure S5(b) illustrated d_{33} and k_p of the ceramics as a function of E_P, measured at T_P=120 ^{o}C. One can see that d_{33} increased sharply when E_P increased from 1.0 kV/mm to 2.0 kV/mm and then increased slowly from 2.0 kV/mm to 6.0 kV/mm, maintaining steadily at a high value of ~520 pC/N. However, k_p increased rapidly when E_P increased from 1.0 kV/mm to 3.0 kV/mm, maintaining at a high level of ~59.3%, demonstrating that electric fields strongly affected piezoelectricity significantly. Based on the results discussed above, we can draw a conclusion that poling temperature as well as electric field can affect piezoelectric behavior.

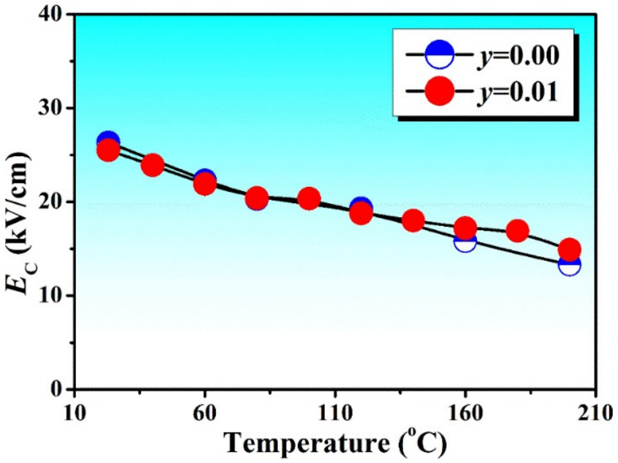

Fig. S6. Evolution of E_C as a function of temperatures in pure BS-PT and BS-PT-0.01BZT samples.

Fig. S6 showed the evolution of E_C as a function of temperatures in BS-PT and BS-PT-0.01BZT ceramics. As one can see, The E_C of both pure BS-PT and BS-PT-0.01BZT samples reduced with increasing temperatures, indicating an easier polarization switching. The decreased E_C may be in favor of the excellent temperature stability for the ceramics. And it can be seen that the E_C values in two components were almost the same. On the one hand, at the low temperature range, we can know from the SS-PFM results [Fig. 6 in manuscript] that the ability of local domain rotation for BS-PT and BS-PT-0.01BZT are similar at high electrical field range, which is consistent with the macroscopic E_C. While the piezoelectric response value of local butterfly loops for BS-PT-0.01BZT was higher than that for BS-PT, indicating stronger domain extension in BS-PT-0.01BZT, which may be responsible for the enhanced macroscopic piezoelectric performance. On the other hand, at the high temperature range, it can be seen from Fig. 7 in manuscript that the majority of domains in BS-PT-0.01BZT ceramics almost remained unchanged, while most domains in pure BS-PT samples disappeared at high temperature. Hence with increasing temperature, the more stable domain structures and similar E_C should lead to the stronger piezoelectric response for BS-PT-0.01BZT than BS-PT under same applied electrical field, consequently resulting in improved temperature stable of piezoelectric properties.

References

1. R. E. Eitel, C. A. Randall, T. R. Shrout and S. E. Park, *Jpn. J. Appl. Phys.*, 2002, **41**, 2099-2104.
2. N. N. Luo, S. J. Zhang, Q. Li, Q. F. Yan, W. H. He, Y. L. Zhang and T. R. Shrout, *Appl. Phys. Lett.*, 2014, **104**, 1804.
3. N. N. Luo, Q. Li, Z. G. Xia and X. C. Chu, *J. Am. Ceram. Soc.*, 2012, **95**, 3246-3253.
4. J. H. Cho, T. K. Song, L. Wang, H. G. Yeo, Y. S. Sung, M. H. Kim and D. S. Park, *J. Appl. Phys.*, 2009, **105**, 061640.
5. K. H. Cho, H. Y. Park, C. W. Ahn, S. Nahm, K. Uchino, S. H. Park, H. G. Lee and H. J. Lee, *J. Am. Ceram. Soc.*, 2007, **90**, 1946-1949.
6. H. C. Song, K. H. Cho, H. Y Park, C. W. Ahn, S. Nahm, K. Uchino, S. H. Park and H. G. Lee, *J. Appl. Phys.*, 2008, **102**, 1812–1816.
7. J. G. Wu, D. Q. Xiao, W. J. Wu, Q. Chen, J. G. Zhu, Z. C. Yang and J. Wang, *J. Eur. Ceram. Soc.*, 2012, **32**, 891-898.
8. S. F. Huang, J. Chang, F. T. Liu, Z. M. Ye and X. Cheng, *J. Mater. Sci.*, 2004, **39**, 6975-6979.